Asia-Pac. J. Atmos. Sci., 51(1), 77-89, 2015
DOI:10.1007/s13143-015-0061-x
pISSN 1976-7633 / eISSN 1976-7951

Projected Change in East Asian Summer Monsoon by Dynamic Downscaling: Moisture Budget Analysis

Chun-Yong Jung*[1], Ho-Jeong Shin[1], Chan Joo Jang[1], and Hyung-Jin Kim[2]

[1]*Physical Oceanography Division, Korea Institute of Ocean Science and Technology, Ansan, Korea*
[2]*Climate Research Department, APEC Climate Center, Busan, Korea*

(Manuscript received 13 August 2014; accepted 19 January 2015)

Abstract: The summer monsoon considerably affects water resource and natural hazards including flood and drought in East Asia, one of the world's most densely populated area. In this study, we investigate future changes in summer precipitation over East Asia induced by global warming through dynamical downscaling with the Weather Research and Forecast model. We have selected a global model from the Coupled Model Intercomparison Project Phase 5 based on an objective evaluation for East Asian summer monsoon and applied its climate change under Representative Concentration Pathway 4.5 scenario to a pseudo global warming method. Unlike the previous studies that focused on a qualitative description of projected precipitation changes over East Asia, this study tried to identify the physical causes of the precipitation changes by analyzing a local moisture budget. Projected changes in precipitation over the eastern foothills area of Tibetan Plateau including Sichuan Basin and Yangtze River displayed a contrasting pattern: a decrease in its northern area and an increase in its southern area. A local moisture budget analysis indicated the precipitation increase over the southern area can be mainly attributed to an increase in horizontal wind convergence and surface evaporation. On the other hand, the precipitation decrease over the northern area can be largely explained by horizontal advection of dry air from the northern continent and by divergent wind flow. Regional changes in future precipitation in East Asia are likely to be attributed to different mechanisms which can be better resolved by regional dynamical downscaling.

Key words: East Asian summer monsoon, dynamical downscaling, pseudo global warming, moisture budget analysis, regional climate change

1. Introduction

The summer monsoon is characterized with heavy rainfall that considerably influences on human life not only by playing as a water resource but also by causing natural hazards such as flood. Under the global warming during the last decades, there has been an increasing trend in precipitation in global monsoon areas (Wang *et al*., 2012, 2013; Hsu *et al*., 2013; IPCC, 2013 and references therein). This increasing trend in precipitation can be attributed to an increase in atmospheric moisture in spite of a weakening of the monsoonal circulations (Ueda *et al*., 2006).

Given the effects on water resources over East Asia, a densely populated agricultural region, it is of considerable importance to project and understand a possible future change in East Asian summer monsoon and its impacts (e.g., Meehl and Arblaster, 2003). Recent studies using a multi-model ensemble that consists of CMIP5 (the fifth phase of Coupled Model Intercomparison Project) global climate models showed an overall increase in summer precipitation over East Asia projected for the late 21st century under RCP (Representative Concentration Pathway) scenarios (Knutti and Sedláèek, 2013; Seo *et al*., 2013).

Although the CMIP5 multi-model ensemble projected an increase in precipitation over East Asia, the individual model results can significantly differ among themselves; in case of RCP4.5 scenario (with 4.5 $W\,m^{-2}$ radiative forcing), some models show an increase and others a decrease especially over inland China (see Fig. 14 in Chen and Sun (2013)). Such an inter-model difference can be related to many factors, but among others, it can be attributed to the global models' inability to adequately capture regional features due to their relatively coarse resolution and insufficient treatment of small scale processes. Most of the CMIP5 models have a horizontal resolution greater than one degree. Despite the continuing improvement in computational resource and power, it is still challenging to use a global model with a high resolution at tens of kilometers for long-term climate simulations. Hence, dynamical downscaling using a regional model has been widely used and even received more attention to support the increasing demand from society on detailed information of regional climate change.

To simulate a regional climate change, a pseudo global warming (PGW hereafter) method was used in this study for dynamical downscaling. This PGW method has been adopted in many studies to reduce a systematic bias in regional climate simulations (e.g., Kimura and Kitoh, 2007; Sato *et al*., 2007; Kawase *et al*, 2009; Yoshikane *et al*., 2012; Morrison *et al*., 2014). The method takes only the difference in climatological mean fields between the present and future climate states

*Current affiliation: Weather Information Service Engine, Center for Atmospheric Sciences and Earthquake Research, Seoul 121-835, Korea.
Corresponding Author: Chan Joo Jang, Physical Oceanography Division, Korea Institute of Ocean Science and Technology, 787 Haean-ro, Sangnok-gu, Ansan 426-744, Korea.
E-mail : cjjang@kiost.ac

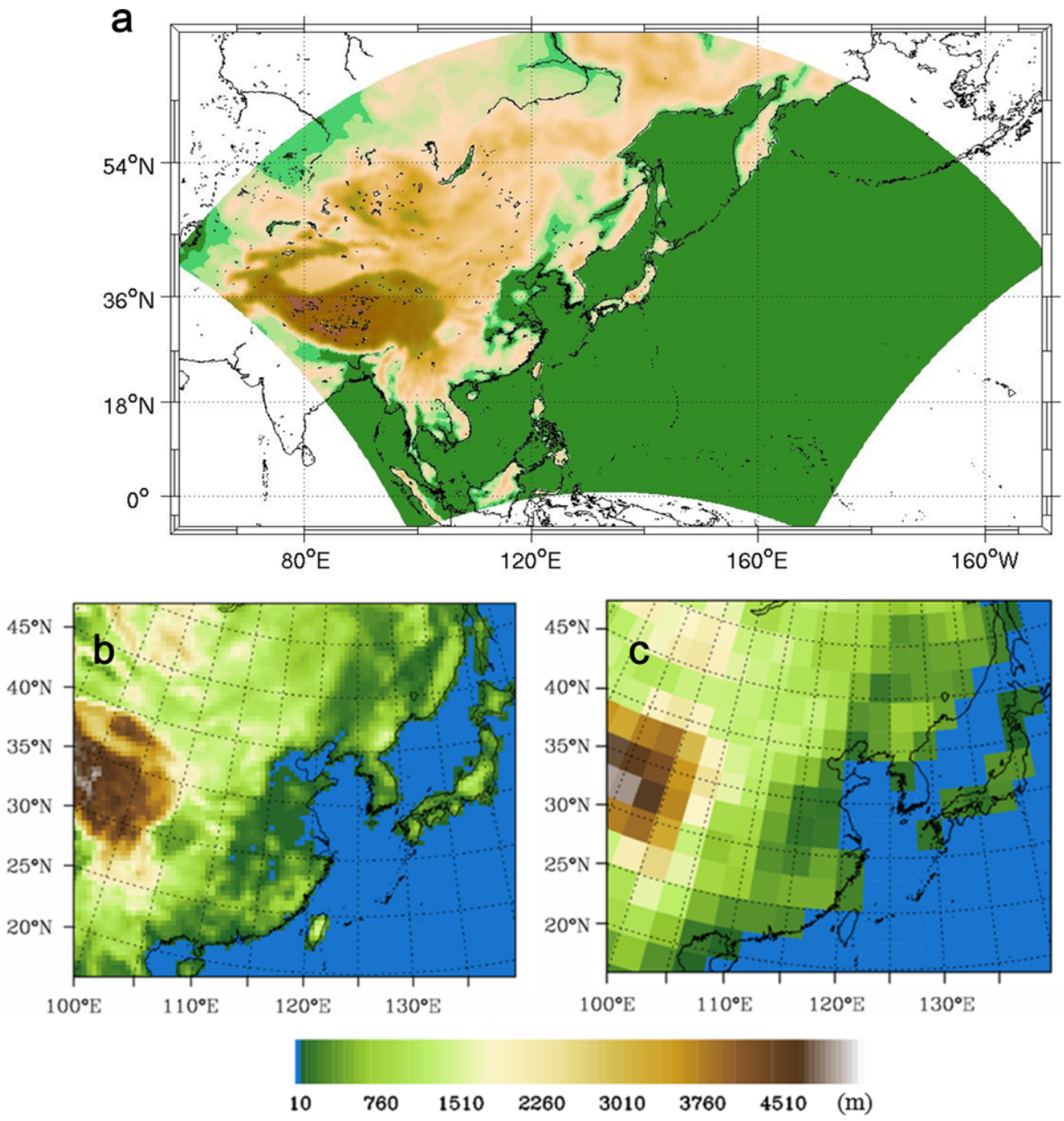

Fig. 1. (a) The experimental domain for dynamical downscaling with WRF, and the model topography in m in our analysis domain for (b) WRF and (c) CanESM2.

simulated by a global climate model and impose it on the observational data, reconstructing a future climate projection. A hindcast simulation using the PGW method was carried out and validated for the Baiu rainfall distribution during the 1960s to 1990s (Kawase *et al*., 2008). Our PGW experiments and the WRF model configuration are described in Section 2.

It is well known that results of dynamical downscaling highly rely on their initial and boundary conditions. For this reason, we have used reanalysis data as the initial and boundary condition to produce a high-resolution data for the present climate. We also conducted an evaluation with CMIP5 global models to select one model that performs better in simulating East Asian summer monsoon for future climate change. For the evaluation, we have devised skill-scores using precipitation and zonal wind at 850 hPa based on multivariate empirical orthogonal function (MVEOF) and correlation coefficient. The equations for the skill-scores and the evaluation results are presented in Section 3.

The purpose of this study is not only to investigate a possible change in East Asian summer monsoon projected under the RCP4.5 global warming scenario using the PGW method, but also to understand its underlying mechanism. There have already been several studies with dynamical downscaling on future change in East Asian summer monsoon, but most of

them analyzed the results with a qualitative approach describing the spatial and temporal patterns of the changes in temperature, precipitation and monsoonal circulation (e.g., Lee *et al*., 2013, 2014; Oh *et al*., 2013, 2014). We further examined the precipitation changes over East Asia and their causal attributions with a quantitative approach by conducting a local moisture budget analysis. A moisture budget analysis has been used to investigate changes in the hydrological cycle due to global warming not only on a global scale (e.g., Watterson, 1998; Hsu *et al*., 2012) but also on a regional scale for East Asia (e.g., Seo *et al*., 2013). They analyzed outputs of global climate models that used the hydrostatic balance equation. Since the Weather Research and Forecasting model (WRF) used for this study is a non-hydrostatic and compressible fluid model, we could decompose a moisture flux into the contributions from moisture advection and wind divergence/convergence. The budget equation is given in Section 2 and its component values and their contributions to a local change in precipitation calculated for the focused areas are presented in Section 4, together with qualitative analysis for the downscaling results for the present and future climate.

In our experimental results, there is a notable regional contrast in the projected summer-mean precipitation change where the Sichuan Basin and Yangtze River are located. A change in precipitation over the Yangtze River has implications in that it can affect the agriculture and cause a flood/drought in the region (Huang *et al*., 2011). It can also affect the river discharge contributing to sea surface warming (Park *et al*., 2011) and to the marine ecosystem variation in the Yellow and East China Seas (Park *et al*., 2014). Our analysis focuses on this regional contrast only for which the moisture budget analysis was conducted.

Table 1. WRF 3.4.1 model configuration and selected physical parameterization schemes.

Configuration	
Map projection	Lambert-conformal
Integration period	0000 UTC 20 April ~ 1800 UTC 31 August
Horizontal resolution	50 km
Number of grid points	215 × 155 × 27
Physical parameterization	
Moist convection	Kain-Fritsch (Kain, 2004)
Microphysics	WSM6 (Hong and Lim, 2006)
Boundary layer	YSU (Hong *et al*., 2006)
Land surface model	Unified Noah (Ek *et al*, 2003)
Shortwave radiation	Dudhia (Dudhia, 1989)
Longwave radiation	RRTM (Mlawer *et al*., 1997)

2. Methodology

a. Pseudo global warming experiment

The WRF version 3.4.1 (Skamarock *et al*., 2008) was used for dynamical downscaling in the PGW experiments. The model was set up on Lambert-conformal map projection with 50 km grid interval. The spatial domain (Fig. 1) chosen for this study covers the whole East Asia (10°S~60°N and 60°E~150°W), including the tropical rain band and westerlies from the Tibetan Plateau. This domain is rather large relative to the domain of our interest. Yoshikane *et al*. (2012) argued that the performance of PGW downscaling highly depended on the modeling domain; for example, precipitation accuracy was

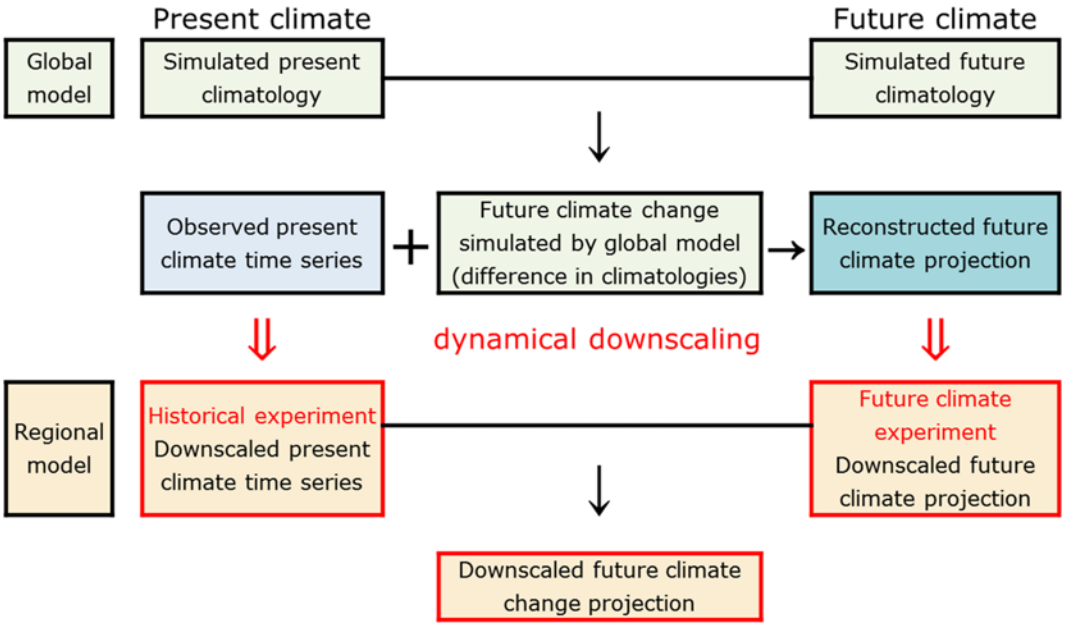

Fig. 2. A schematic diagram of the pseudo global warming experiment with dynamical downscaling for a future climate projection.

Table 2. List of CMIP5 global models evaluated for East Asian summer monsoon and their approximated horizontal resolution.

Model I.D.	Modeling Center	Resolution
BCC-CSM1-1	Beijing Climate Center, China Meteorological Administration	$2.8^o \times 2.8^o$
BCC-CSM1-1-M	Beijing Climate Center, China Meteorological Administration	$1.1^o \times 1.1^o$
BNU-ESM	Beijing Normal University	$2.8^o \times 2.8^o$
CMCC-CESM	Centro Euro-Mediterraneo sui Cambiamenti Climatici (Euro-Mediterranean Center on Climate Change)	$3.8^o \times 3.8^o$
CMCC-CM	Centro Euro-Mediterraneo sui Cambiamenti Climatici (Euro-Mediterranean Center on Climate Change)	$0.8^o \times 0.8^o$
CMCC-CMS	Centro Euro-Mediterraneo sui Cambiamenti Climatici (Euro-Mediterranean Center on Climate Change)	$1.9^o \times 1.9^o$
CNRM-CM5	Centre National de Recherches Météorologiques / Centre Européen de Recherche et Formation Avancée en Calcul Scientifique	$1.4^o \times 1.4^o$
CanCM4	Canadian Centre for Climate Modelling and Analysis	$2.8^o \times 2.8^o$
CanESM2	Canadian Centre for Climate Modelling and Analysis	$2.8^o \times 2.8^o$
FIO-ESM	The First Institute of Oceanography, SOA, China	$2.8^o \times 2.8^o$
HadCM3	Met Office Hadley Centre	$3.8^o \times 2.5^o$
MPI-ESM-LR	Max-Planck-Institut für Meteorologie (Max Planck Institute for Meteorology)	$1.9^o \times 1.9^o$
MPI-ESM-MR	Max-Planck-Institut für Meteorologie (Max Planck Institute for Meteorology)	$1.9^o \times 1.9^o$
MPI-ESM-P	Max-Planck-Institut für Meteorologie (Max Planck Institute for Meteorology)	$1.9^o \times 1.9^o$
NorESM1-M	Norwegian Climate Centre	$2.5^o \times 1.9^o$
NorESM1-ME	Norwegian Climate Centre	$2.5^o \times 1.9^o$

reduced near the upstream side of lateral boundaries with a small domain. In this study, we confined our analysis to a smaller domain, approximately 20°N~50°N and 100°E~140°E (the inner domain in Fig. 1). The model configurations are summarized in Table 1 with further specifications on physical parameterizations.

As a baseline (CTRL hereafter) of the PGW experiment, NCEP/DOE (National Centers for Environmental Prediction/ Department of Energy) global reanalysis data (Kanamitsu *et al*., 2002) were downscaled with WRF from 1981 to 1990. Starting the downscale simulation on 0000 UTC of April 20th each year, we regridded the NCEP/DOE reanalysis data onto the WRF grids with a bi-linear method and used the regridded data at the corresponding date and time as its initial condition. The reanalysis data were also input to the model as the lateral boundary condition every six hours throughout the entire simulation. A previous study using the PGW method conducted a baseline simulation separately for the 1980s and 1990s and found no significant difference in the resultant precipitation changes (Kawase *et al*., 2009). This suggests that the PGW experiment results for a climate change may be sensitive not to its baseline simulation period but to the projected climatological mean differences used as input.

For downscaling of future climate projection, we calculated six-hourly climatological mean differences between the CanESM2 (r1i1p1) RCP4.5 output for years 2081 to 2100 and its corresponding Historical output for years 1981 to 2000. The CanESM2 outputs were linearly interpolated to six-hour interval whenever needed and also regridded onto the WRF grids with bi-linear interpolation. By adding the CanESM2 climatological mean differences to the six-hourly time-series of NCEP/DOE reanalysis for years 1981 to 1990, we constructed a climatological projection dataset with a ten-year ensemble. The PGW downscaling experiment (PGW_CanESM2 hereafter) was then carried out for the ten years from 1981 to 1990 using the climatological projection for the late 21st century climate. In order to reduce the computational burden, the CTRL and PGW_CanESM2 were carried out only for an extended period of summer from April 20th to August 31st (11 days for spin-up and 123 days from May to August for analysis) every year during the ten years. A schematic diagram summarizing this PGW experimental design is shown in Fig. 2.

Since the PGW method takes only the climatological mean field to represent a climate change, one major limitation would be that the changes in temporal variabilities are excluded (Kawase *et al*., 2008). Thus, this constraint should be considered when planning a PGW experiment and interpreting the results.

b. Moisture budget equation

By ignoring the horizontal diffusion of moisture and the amount of water in liquid and ice phases in the air, Trenberth and Guillemot (1995) used an air-column moisture budget equation for their global atmospheric water budget analysis given as:

$$\frac{\partial W_A}{\partial t} + \vec{\nabla} \cdot \frac{1}{g} \int_{p_s}^{0} q \vec{V} dp = E - P \,, \tag{1}$$

where W_A is column-integrated water vapor (i.e., precipitable water), g the gravitational acceleration, p air pressure, $\vec{V}$ horizontal wind vector, q specific humidity, p_s, E, and P air pressure, evaporation, and precipitation rate at the surface, respectively. The first term on the left hand side, a precipitable

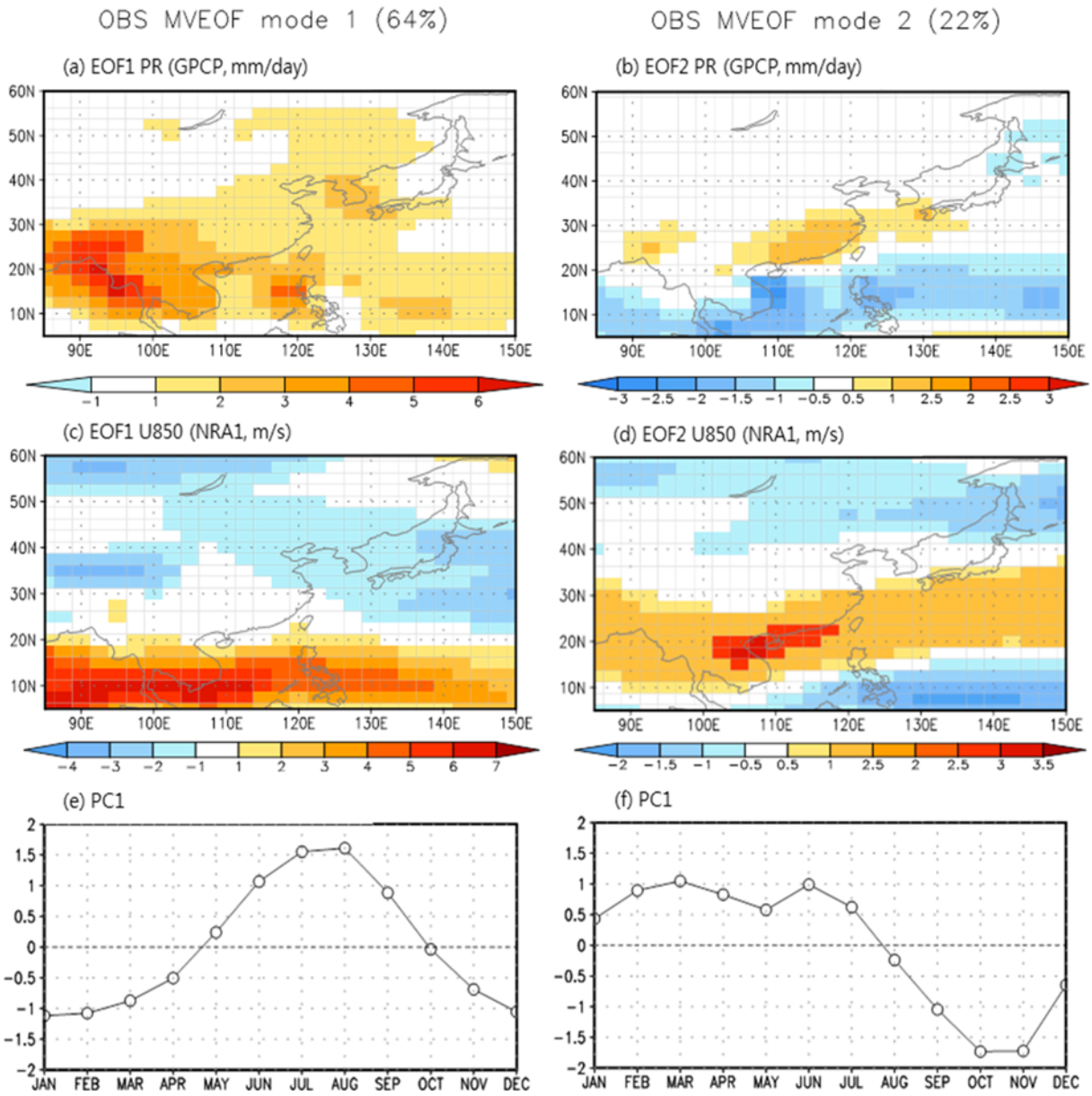

Fig. 3. The first (left) and second (right) leading MVEOF modes and their fractional variances obtained from GPCP precipitation and NCEP/NCAR zonal wind at 850 hPa. See the text for more details.

water tendency, is the atmospheric storage rate of column-integrated water vapor. This water vapor storage rate varies with season, but the rate is negligible in an annual mean or within a season. A previous study (Seo *et al.*, 2013) that analyzed a moisture budget for East Asian summer monsoon using CMIP5 global model data ignored the storage rate and used monthly mean values to calculate the other terms in Eq. (1). They regarded all other contributing factors to the moisture budget as the residual R. The residual thus includes sub-monthly contributions. Their simplified budget equation using monthly mean values is then

$$\langle \vec{\nabla} \cdot \left(\overline{q\vec{V}} \right) \rangle = \overline{E} - \overline{P} + R \,, \tag{2}$$

where < > denotes vertical integration within an air column, and the overbar monthly average.

Focusing on the regional precipitation change and aiming to investigate the causal attributions of the change, we decomposed the moisture transport in flux form on the left hand side of Eq. (2) into the horizontal advection of moisture and the moisture flux by wind divergence as done by Hsu *et al.* (2012). To include their submonthly transient effects of each term in the moisture budget equation, we calculated the monthly mean values for each term with three-hourly WRF outputs. Our budget equation is then

$$\overline{\langle \vec{V} \cdot (\vec{\nabla} q) \rangle} + \overline{\langle q \vec{\nabla} \cdot \vec{V} \rangle} = \overline{E} - \overline{P} + \varepsilon \,, \tag{3}$$

where ε is a residual that includes the neglected horizontal diffusion of moisture and a numerical truncation error. For the purpose of causal attribution of a future change (Δ) in precipitation, the terms in Eq. (3) can be re-arranged as follows:

$$\Delta\overline{P} = \Delta\overline{E} - \Delta\overline{\langle \vec{V}\cdot(\vec{\nabla}q)\rangle} - \Delta\overline{\langle q\vec{\nabla}\cdot\vec{V}\rangle} + \Delta\varepsilon. \quad (4)$$

Prior to the calculation, the original WRF output was regridded onto regular latitude-longitude grids and vertically onto pressure levels with an official WRF post-processing package, ARWpost[1].

3. Evaluation of the CMIP5 models for East Asian summer monsoon

Regional modeling results heavily rely on the inputs from global model simulation (e.g., Chen and Sun, 2009; Kawase *et al*., 2009; Adachi *et al*., 2012). Selection of a global model is thus crucial for dynamical downscaling with a regional model. Under the assumption that a model bias against observation is steady and insensitive to the climate forcings, the models with a better capability of simulating the present/past climate are supposed to better project future climate changes. Although it may not be absolutely true, we evaluated CMIP5 global models for East Asian summer monsoon against observational data and selected only one model as our first attempt for PGW downscaling.

Typically, East Asian summer monsoon is characterized by heavy rainfall and a seasonal reversal of surface wind direction. Thus, to evaluate the East Asian summer monsoon simulated by the global models, we used precipitation and zonal wind at 850 hPa from the CMIP5 Historical simulation outputs regridded onto a uniform grid system of $2.5^{o} \times 2.5^{o}$. Similar to the method in Wang *et al*. (2008), we performed a MVEOF analysis for each model using the forty-year monthly climatology from 1961 to 2000. The spatial domain chosen for the analysis is 85°E~150°E and 5°N~60°N that includes the East Asian continent and the Northwest Pacific Ocean.

Among the CMIP5 models available for the Historical outputs, sixteen models (Table 2) that had provided a complete dataset for the zonal wind without a missing value below the terrain surface at 850 hPa were used for this analysis and evaluation.

The observational data used to evaluate the global models are the precipitation rate from GPCP (Global Precipitation Climatology Project) dataset (Huffman *et al*., 2011) from 1979 to 2010 and the zonal wind from NCEP/NCAR (National Center for Environmental Prediction/National Center for Atmospheric Research) reanalysis data (Kalnay *et al*., 1996) from 1961 to 2000. The observational data periods are not consistent with each other, but they were chosen to obtain a climatology with a longer time period depending on the data availability. Figure 3 shows the first two leading eigen vectors and principal components from the MVEOF analysis performed with the observational data. These modes account for 64% and 22% of the total variance, respectively, representing the summer-winter and the spring-fall contrast due to the seasonal reversal of winds.

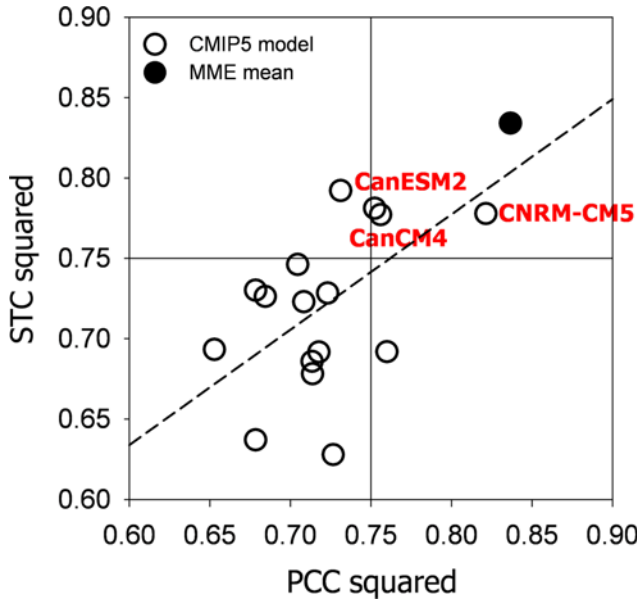

Fig. 4. Scatter diagram displaying squared skill-scores for East Asian summer monsoon simulated by CMIP5 global models with spatiotemporal correlation (STC) and the year-average of monthly-calculated spatial pattern correlation (PCC). Open circles represent the individual model results, and the solid circle represents their ensemble mean.

For model evaluation, we have devised a skill score (SC) with spatial pattern correlation using the MVEOF eigenvectors of precipitation (PREOF) and zonal wind at 850 hPa (U850EOF) and another (TC) with temporal correlation using their corresponding principal components (PC). Both of the scores are the averages of the two modes with correlation coefficients between the global model data and the observational data weighted by the observed fractional variance. As such,

$$SC = \frac{0.64\left(\frac{PREOF1 + U850EOF1}{2}\right) + 0.22\left(\frac{PREOF2 + U850EOF2}{2}\right)}{0.64 + 0.22}, \quad (5)$$

$$TC = \frac{0.64PC1 + 0.22PC2}{0.64 + 0.22}. \quad (6)$$

Then, the evaluation was done with their combined score (STC), a new skill-score with spatiotemporal correlation, given in Eq. (7):

$$STC = \frac{SC \times DOFS + TC \times DOFT}{DOFS + DOFT}. \quad (7)$$

Here, DOFS is the number of grids and DOFT is the length of the time series used to calculate the correlation coefficients.

[1]http://www2.mmm.ucar.edu/wrf/OnLineTutorial/Graphics/ARWpost/index.html

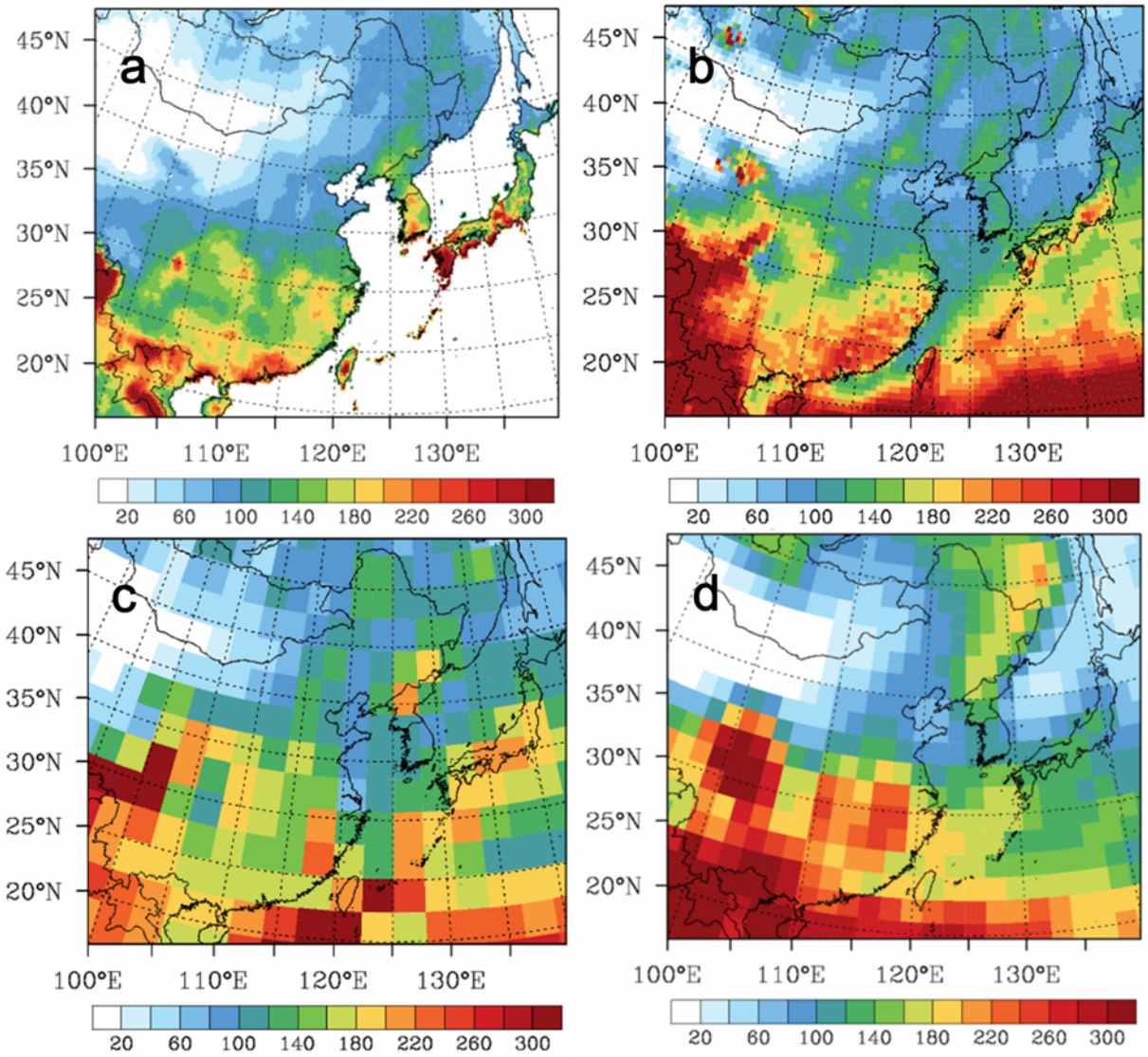

Fig. 5. Climatological summer (May to August) mean precipitation in mm mo^{-1} for 1981 to 1990: (a) APHRODITE high-resolution observational data, (b) CTRL downscaling results with WRF, (c) CanESM2 CMIP5 Historical output, and (d) NCEP/DOE reanalysis data.

STC is an average of SC and TC weighted by the degree of freedom in space (DOFS) and in time (DOFT).

In addition to STC, the arithmetic average of the pattern correlation coefficients (PCCs) for each month of the year was calculated using climatological monthly mean fields for precipitation and 850 hPa zonal wind. While the MVEOF was performed to particularly assess the seasonal variation, this monthly pattern correlation was calculated to assess the overall similarity in normal spatial pattern of the model data to the observational data.

The results calculated for each of the sixteen models are shown as a scatter plot in Fig. 4 with the square of STC on the ordinate and the square of PCC on the abscissa. Plotting the squared skill scores in the figure was designed to mimic R-square as a measure of goodness-of-fit. In addition, it makes the scores greater than 0.5 more dispersive and easier to distinguish among themselves. The scatter plot indicates that CanESM2, CanCM4, and CNRM-CM5 have the highest skill scores in simulating East Asian summer monsoon. Finally, as our first attempt for PGW downscaling, we have selected one model, CanESM2, which reduced our computational burden.

4. Pseudo global warming experiment results

a. Precipitation and surface air temperature for the present climate

The CTRL precipitation downscaled from the NCEP/DOE reanalysis data is shown in Fig. 5 for climatological summer mean precipitation. To validate the downscaling results, observational precipitation data from APHRODITE (Asian Precipitation-Highly-Resolved Observational Data Integration Towards

Table 3. Mean biases and spatial pattern correlation coefficients using summer (May to August) mean climatology for 1981 to 1990 over the land area of East Asia for surface air temperature and precipitation rate. The observational data consist of APHRODITE precipitation at a quarter degree and ERA-interim temperature at a half degree. Based on the observational data set, the biases and correlations with CTRL downscaled with WRF, the NCEP/DOE reanalysis used for the downscaling, and CanESM2 CMIP5 Historical output have been calculated after regridding onto the CanESM2 resolution (~2.8° × 2.8°) that is coarsest among these data.

Variable	Data	Bias	Correlation
2 m air temperature (°C)	CTRL	0.03	0.99
	NCEP/DOE	0.70	0.98
	CanESM2	1.61	0.98
Precipitation rate (mm mo^{-1})	CTRL	36.3	0.90
	NCEP/DOE	41.1	0.81
	CanESM2	11.3	0.83

Evaluation) at a quarter degree is shown in Fig. 5a for land area of the analysis domain. The CanESM2 global model data as well as the NCEP/DOE reanalysis that were used as the input for CTRL are also shown in the figure for comparison. The heavy rainfall pattern in CTRL (Fig. 5d) was similar to the NCEP/DOE analysis, but with reduced overestimation over the southern China. For example, the mean bias averaged over land area of the analysis domain was reduced by about 5 mm mo^{-1} from 41.1 to 36.3 mm mo^{-1} as shown in Table 3. In the table, the spatial pattern correlation coefficient calculated with the APHRODITE climatology for land area is 0.90 which is 0.09 higher than 0.81 for NCEP/DOE reanalysis. Regarding monsoonal heavy rainfall in East Asia, CTRL produced the Meiyu-Baiu rain band along the Yangtze River basin around 30°N across Central and East China reaching over Japan, but it underestimated the Changma rainfall over the Korean Peninsula. The bias calculated with CanESM2 against APHRODITE was 11.3 mm mo^{-1} which is smaller than a third of the CTRL bias, which agrees to a previous result that global models tend to underestimate rainfall intensity as compared with regional models (Kusunoki and Arakawa, 2012; Seo and Ok, 2013; Seo *et al*., 2013). The CanESM2 pattern correlation coefficient was 0.83 which is lower than the CTRL result by 0.07 and slightly

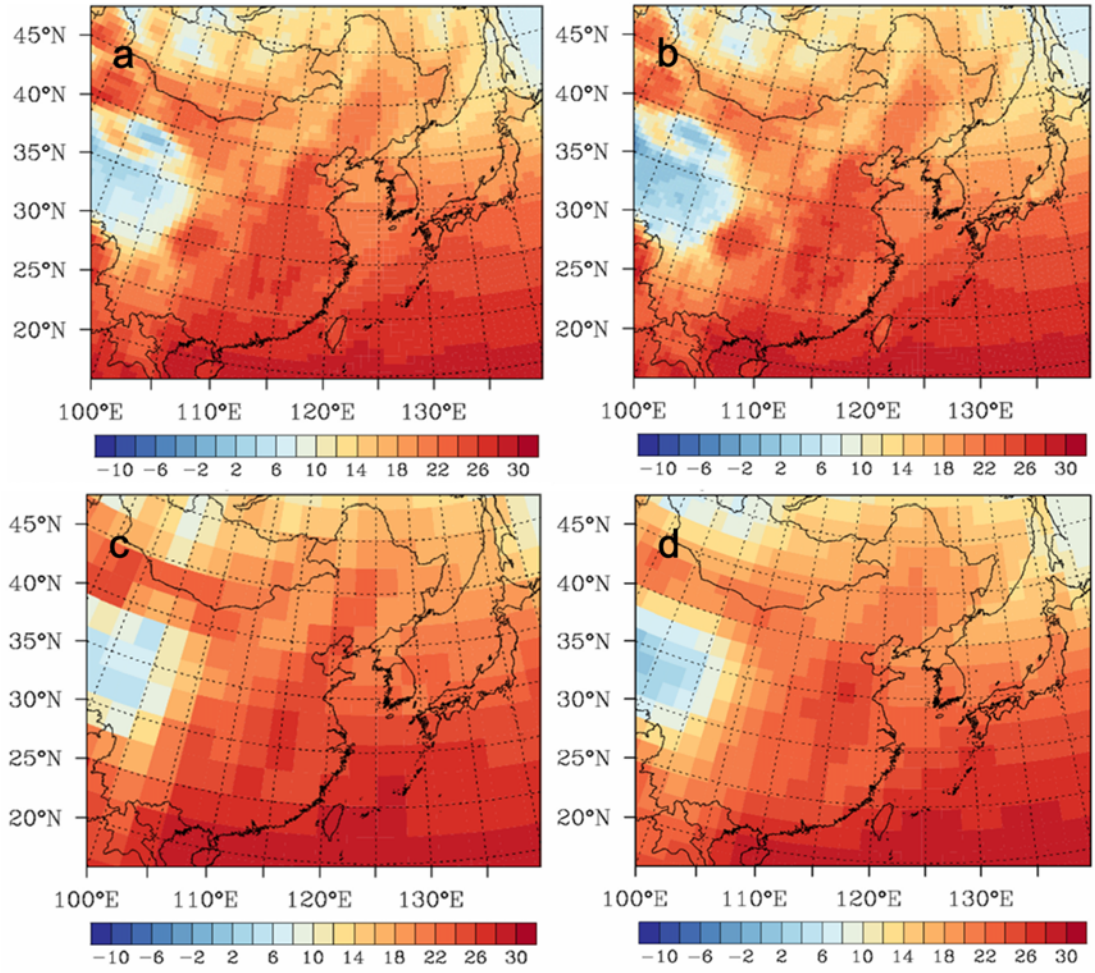

Fig. 6. Climatological summer (May to August) mean surface air temperature in °C for 1981 to 1990: (a) ERA-interim reanalysis data at a half-degree, (b) CTRL downscaling results with WRF, (c) CanESM2 CMIP5 Historical output, and (d) NCEP/DOE reanalysis data used as input for the CTRL downscaling.

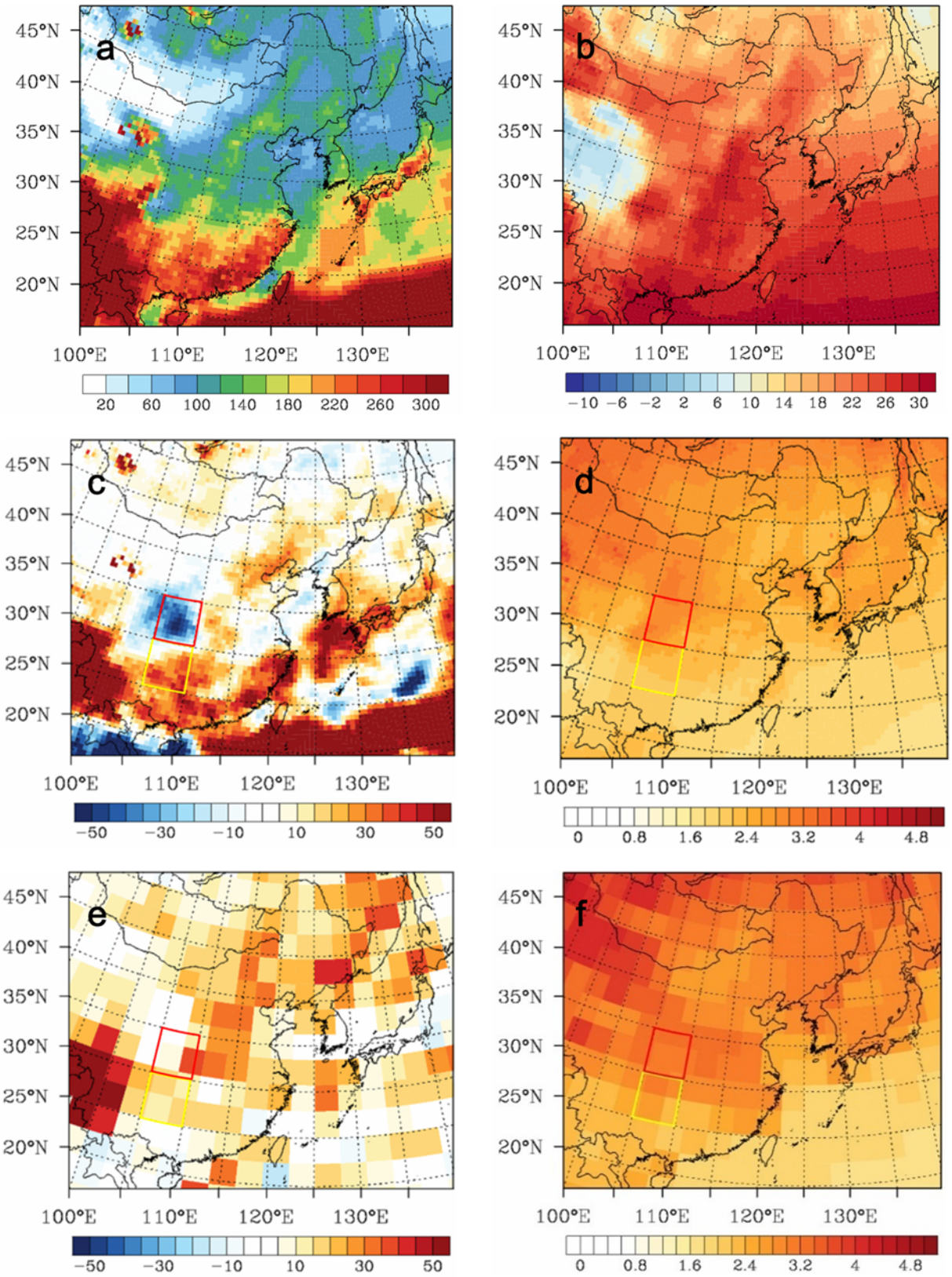

Fig. 7. Climatological summer (May to August) mean precipitation in mm mo^{-1} (left) and surface air temperature in ^{o}C (right): (a, b) PGW_CanESM2 pseudo global warming experiment downscaled with WRF, (c, d) the difference in the PGW_CanESM2 and the CTRL downscaling outputs, and (e, f) the difference in CanESM2 CMIP5 RCP4.5 climatology for 2081 to 2100 and Historical climatology for 1981 to 2000. Boxes in (c)-(f) denote the areas where the mositure budget was analyzed.

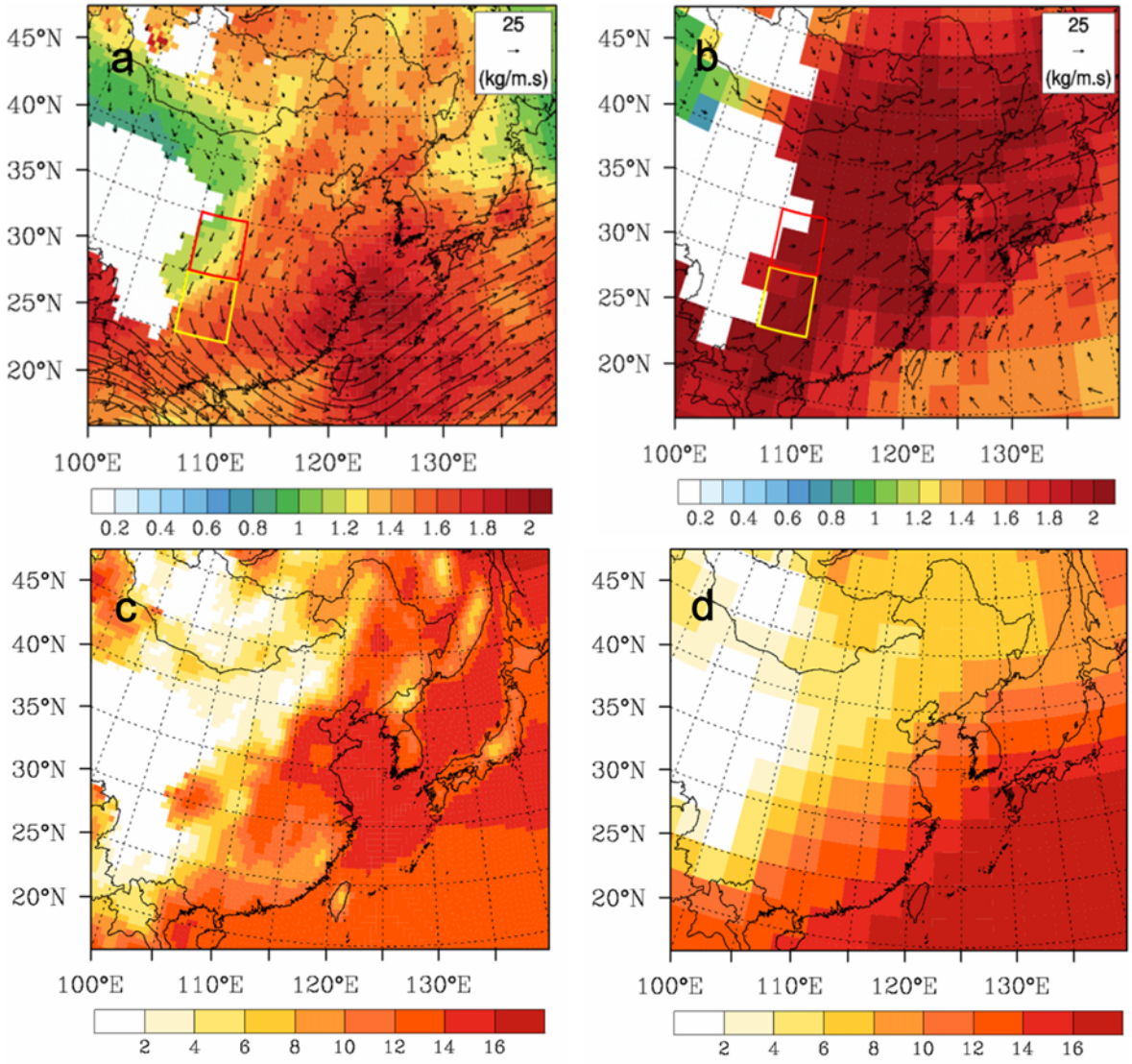

Fig. 8. Summer mean specific humidity (color shaded) at 850 hPa in kg kg^{-1} and superimposed vertically integrated moisture flux (arrows) in kg m^{-1} s^{-1} in the upper panels and geopotential height (color shaded) at 850 hPa in m in the lower panels: (a, c) a future change obtained from the PGW_CanESM2 minus CTRL climatology and (b, d) that from CanESM2 CMIP5 RCP4.5 minus Historical climatology. Non-colored area represents the area with terrain height above 850 hPa.

higher than the NCEP/DOE result.

Climatological summer-mean surface air temperature is shown in Fig. 6 for CTRL with ERA-interim (European Center for Medium-range Weather Forecast Reanalysis-Interim) reanalysis data at a half degree. CanESM2 global model data and the NCEP/DOE reanalysis data used for the downscaling are also shown in the figure for comparison. These four data sets all show a considerably similar pattern and magnitude in temperature: colder over the Tibetan Plateau and the Sea of Okhotsk and warmer over East China including the East China Sea where southerly wind along the western boundary of North Pacific high transport hot and humid air. The downscaled CTRL presented more detailed regional structure of temperature pattern compared with CanESM2 global model and NCEP/DOE reanalysis data. Particularly, a relatively high temperature core in Sichuan Basin located at the eastern foothills of the Tibetan Plateau was captured in CTRL (Fig. 6b), as appeared in the ERA-interim data (Fig. 6a). Our results confirm that a regional model with dynamical downscaling can better simulate temperature rather than precipitation (e.g., Chang and Hong, 2011; Sun *et al*., 2011; Sales and Xue, 2012).

b. Projected changes in precipitation and surface air temperature

PGW_CanESM2 results are shown in Fig. 7 for climatological summer mean precipitation and surface air temperature for the late 21st century (2081~2100) under RCP4.5 scenario. The differences from the CTRL results for the present climate (Figs. 7c, d) and the projected changes by CanESM2 (Figs. 7e,

f) are also shown in the figure. The overall increase in precipitation and temperature projected by CanESM2 agrees to the future climate changes over East Asia simulated by CMIP5 multiple models (IPCC, 2013).

The temperature change pattern shown in Figs. 7d, f can be summarized as "warmer in high latitudes and inland with global warming". Such a warming pattern could possibly have contributed to the moistening of low-level atmosphere as shown in Figs. 8a, b, following the Clausius-Clapeyron relation (Held and Soden, 2006). This relation between surface warming and moistening may support that the lesser atmospheric warming by PGW_CanESM2 would have caused a lesser moistening of the low-level atmosphere as compared with CanESM2 especially over land areas. Although the surface temperature change projected by CanESM2 was input for the PGW_CanESM2 downscaling simulation, the surface air temperature (i.e., temperature at 2 m above the surface) projected by PGW_CanESM2 could differ from the CanESM2 projection, affected by various factors such as changes in low-level pressure, regional circulation, and atmospheric stability.

As for the projected precipitation change, both of CanESM2 and PGW_CanESM2 increased the moisture flux passing over the East China Sea from the Southwest, but the moisture flux in the CanESM2 result was more inland. As shown in the right panels of Fig. 8, in CanESM2, the change in vertically-integrated moisture flux caused the increase in precipitation over East Asia due to an intensification of the subtropical North Pacific high and southwesterly wind along the western boundary of the high, in consistent with a previous study with multiple CMIP5 global models (Seo *et al*., 2013).

Unlike the overall increase simulated by CanESM2 (Fig. 7e), PGW_CanESM2 reduced precipitation at the local areas over Southwest China and Vietnam while it increased precipitation near the coast of the southern China and along the Meiyu-Baiu and Changma areas. In Southwest China, the precipitation is projected to be decreased in a northern area (indicated as a red box in Fig. 7) while it is projected to be increased in its southern area (indicated as a yellow box in Fig. 7) through which the Yangtze River flows. The left panels in Fig. 8 illustrate that in PGW_CanESM2, cold and dry air was transported from the northern continent to the south and merged with hot and humid air from the subtropical Pacific. This cold and dry inflow from the north might have caused the precipitation decrease in the northern area. As the air passing over the Yangtze River, surface evaporation in the southern area would have been increased due to ventilation and water supply from the river. Because of this southward intrusion of continental flow, the moisture flux from the Southwest along the subtropical North Pacific high appears to be confined to the East China Sea having little influence over inland China. To further examine the causal attribution of these regionally contrasting changes in precipitation over the Southwest China region, we analyzed an atmospheric moisture budget averaged over the local areas and present the results in the following section.

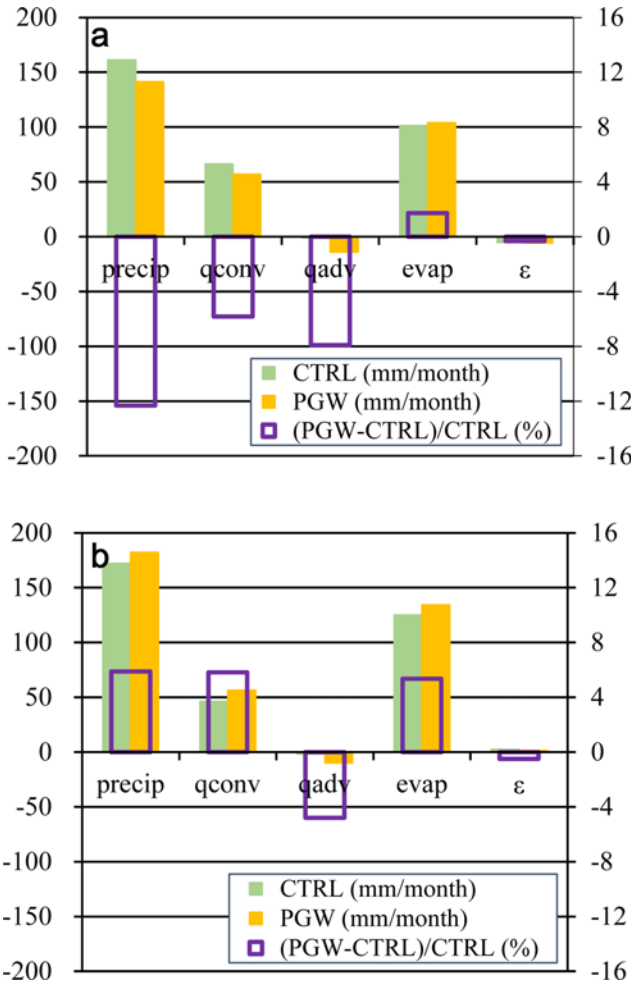

Fig. 9. Moisture budget terms calculated from the pseudo global warming experiments for a future climate averaged for 2081 to 2100 (PGW_CanESM2) and the downscaling result from NCEP/DOE reanalysis for the present climate averaged for 1981 to 2000 (CTRL): (a) the results averaged over the northern area of 105°E~110°E and 30°N~35°N and (b) those averaged over the southern area of 105°E~110°E and 25°N~30°N. Green and yellow bars respectively denote the CTRL and PGW_CanESM2 results in mm mo^{-1} with the scale at left. Purple boxes denote their differences in percent with the scale at right.

c. Moisture budget analysis for the regional precipitation change

Although we tried to explain the opposite changes in precipitation over the indicated areas with the aid of analyzing moisture flux and geopotential height, it is still unclear why the precipitation change pattern was contrasted in these areas. Thus, we conducted a quantitative analysis by calculating the area-averaged, vertically-integrated atmospheric moisture budget for each of the indicated areas.

Figure 9 illustrates the moisture budget terms in Eq. (4). The precipitation decrease in the northern area, despite a slight increase in surface evaporation, can be attributed primarily to the horizontal advection of relatively dry air from the north continental area as discussed above and secondarily to the

divergent wind flow (Fig. 9a). In the mean time, the precipitation increase in the southern area, despite the dry air advection from the north, can be attributed to the increase in convergent wind flow and surface evaporation overly compensating the dry advection (Fig. 9b). A strengthened wind could drive more evaporation from the surface through ventilation and a convergent flow would make the water vapor stay locally. The approximately twice larger evaporation increment in the southern area than the increment in the northern area can be explained by the geographic feature that the Yangtze River could supply water vapor to the atmosphere.

5. Conclusions

The purpose of this study was to investigate summer precipitation change in East Asia projected under the RCP4.5 global warming scenario by using the PGW method and to understand its underlying mechanism. Unlike the previous studies on East Asian monsoon that focused on a qualitative description of projected changes in precipitation, we additionally tried to identify the physical causes of the precipitation change under global warming by analyzing a local moisture budget. Focused on a significant contrast in precipitation change in the Southwest China, the moisture budget analysis indicated that an increase in horizontally convergent wind and surface evaporation led to the precipitation increase over the southern area, while a horizontal advection of dry air from the northern continent led to the precipitation decrease over the northern area.

This regionally contrasting change does not appear in the CanESM2 global model result and in other CMIP5 global model results as well (IPCC, 2013), indicating that such regional-scale change may be poorly resolved by global models at low resolution. Most of the CMIP5 models have an atmospheric component at one or larger degree resolution. The average resolution of 47 atmospheric components that we have collected is about 2.2 degrees. Contrary to the results from the global models, a recent domestic report with dynamical-downscaling using HadGEM3-RA regional model includes a figure displaying a similar, contrasting pattern in the precipitation change (Fig. 5.8 in NIMR, 2012). Yet, they did not mention the pattern in the report without in-depth analysis. Our analysis with local moisture budget may provide an example of a quantitative approach to investigate the causal attributions for such hydrological changes on a regional scale.

For this study, we used only one global model data with RCP4.5 scenario for the pseudo global warming experiments to investigate a future change in East Asian summer monsoon, focusing on precipitation change and the moisture budget related to the change. By using multiple models, it can be possible to assess the uncertainty of the future projection, which would be one of our future research.

Acknowledgments. This research was a part of the project (PM58210) titled "Development of coastal erosion control technology", funded by the Ministry of Oceans and Fisheries in Korea, and was funded by the Korea Meteorological Administration Research and Development Program under grant CATER 2012-3052. H.-J. Kim acknowledges the support from APEC Climate Center. We also acknowledge the support by the Supercomputing Center/Korea Institute of Science and Technology Information with supercomputing resources including technical support (KSC-2012-C1-16 and KSC-2013-C2-056) and the World Climate Research Programme's Working Group on Coupled Modelling, which is responsible for CMIP, and we thank the climate modeling groups for producing and making available their model output. For CMIP the U.S. Department of Energy's Program for Climate Model Diagnosis and Intercomparison provides coordinating support and led development of software infrastructure in partnership with the Global Organization for Earth System Science Portals. We especially thank the anonymous reviewers for their helpful comments.

Edited by: John McGregor

REFERENCES

Adachi, S. A., F. Kimura, H. Kusaka, T. Inoue, and H. Ueda, 2012: Comparison of the impact of global climate changes and urbanization on summertime future climate in the Tokyo metropolitan area. *J. Appl. Meteor. Climatol*., **51**, 1441-1454.

Chang, E. C., and S.-Y. Hong, 2011: Projected climate change scenario over East Asia by a regional spectral model. *J. Korean Earth Sci. Soc.*, **32**, 770-783.

Chen, H. P., and J. Q. Sun, 2009: How the "best" models project the future precipitation change in China. *Adv. Atmos. Sci*., **26**, 773-782.

_____, and _____, 2013: Projected change in East Asian summer monsoon precipitation under RCP scenario. *Meteor. Atmos. Phys*., **121**, 55-77.

Dudhia, J., 1989: Numerical study of convection observed during the winter monsoon experiment using a meso-scale two-dimensional model. *J. Atmos. Sci*., **46**, 3077-3107.

Ek, M. B., K. E. Mitchell, Y. Lin, E. Rogers, P. Grunmann, V. Koren, G. Gayno, and J. D. Tarpley, 2003: Implementation of Noah land surface model advances in the national centers for environmental prediction operational mesoscale Eta model. *J. Geophys. Res.*, **22**, 8851, doi:10.1029/2002JD003296.

Held, I. M., and B. J. Soden, 2006: Robust responses of the hydrological cycle to global warming. *J. Climate*, **19**, 5686-5699.

Hong, S. Y., and J.-O. Lim, 2006: The WRF single-moment microphysics scheme (WSM6). *J. Korean Meteor. Soc*., **42**, 129-151.

_____, Y. Noh, and J. Dudhia, 2006: A revised vertical diffusion package with an explicit treatment of entrainment processes. *Mon. Wea. Rev*., **134**, 2318-2341.

Hsu, P.-C., T. Li, H. Murakami, and A. Kitoh, 2013: Future change of the global monsoon revealed from 19 CMIP5 models. *J. Geophys. Res. Atmos*., **118**, 1247-1260.

Huang, J., J. Zhang, Z. Zhang, C. Xu, B. Wang, and J. Yao, 2011: Estimation of future precipitation change in the Yangtze River basin by using statistical downscaling method. *Stoch. Env. Res. Risk A.*, **25**(6), 781-792.

Huffman, G. J., D. T. Bolvin, and R. F. Adler, 2011: Global precipitation climatology project version 2.2 combined precipitation data set. world data center A, national climatic data center, Asheville, NC. [Available

online at http://www.ncdc.noaa.gov/oa/wmo/wdcamet-ncdc.html]

IPCC, 2013: Climate Change 2013: The Physical Science Basis. Contribution of Working Group I to the Fifth Assessment Report of the Intergovernmental Panel on Climate Change [Stocker, T. F., D. Qin, G.-K. Plattner, M. Tignor, S. K. Allen, J. Boschung, A. Nauels, Y. Xia, V. Bex, and P. M. Midgley (eds.)]. Cambridge University Press, Cambridge, United Kingdom and New York, NY, USA, 1535 pp.

Kain, J. S., 2004: The Kain-Fritsch convective parameterization: An update. *J. Appl. Meteor*., **43**, 170-181.

Kalnay, E., and Coauthors, 1996: The NCEP/NCAR 40-Year Reanalysis Project. *Bull. Amer. Meteor.Soc.*, **77**, 437-471.

Kanamitsu, M., W. Ebisuzaki, J. Woollen, S.-K. Yang, J. J. Hnilo, M. Fiorino, and G. L. Potter, 2002: NCEP-DOE AMIP-II Reanalysis (R-2). *Bull. Amer. Meteor. Soc*., **83**, 1631-1643.

Kawase, H., T. Yoshikane, M. Hara, B. Ailikun, F. Kimura, and T. Yasunari, 2008: Downscaling of the climatic change in the Mei-yu rainband in East Asia by a pseudo climate simulation method. *Sci. Online Lett. Atmos.*, **4**, 73-76.

_____, _____, _____, F. Kimura, T. Yasunari, B. Ailikun, H. Ueda, and T. Inoue, 2009: Intermodel variability of future changes in the Baiu rainband estimated by the pseudo global warming downscaling method. *J. Geophys. Res*., **114**, D24110, doi:10.1029/2009JD011803.

Kimura, F., and A. Kitoh, 2007: Downscaling by pseudo global warming method. Final Rep., pp. 43-46, ICCAP, Res. Inst. for Humanity and Nat., Kyoto, Japan.

Knutti, R., and J. Sedláček, 2013: Robustness and uncertainties in the new CMIP5 climate model projections. *Nature Climate Change*, **3**, 369-373.

Kusunoki, S., and O. Arakawa, 2012: Change in the precipitation intensity of the East Asian summer monsoon projected by CMIP3 models. *Clim, Dynam*., **38**, 2055-2072

Lee, D. K, D. H. Cha, C. S. Jin, and S. J. Choi, 2013: A regional climate change simulation over East Asia. *Asia-Pac. J. Atmos. Sci*., **49**, 655-664.

Lee, J. W., S.-Y. Hong, E. C. Chang, M. S. Suh, and H. S. Kang, 2014: Assessment of future climate change over East Asia due to the RCP scenarios downscaled by GRIMs-RMP. *Clim. Dynam.*, **42**,733-747.

Meehl, J., and M. Arblaster, 2003: Mechanisms for projected future changes in south Asian monsoon precipitation. *Clim. Dynam*., **21**, 659-675.

Mlawer, E. J., S. J. Taubman, P. D. Brown, M. J. Iacono, and S. A. Clough, 1997: Radiative transfer for inhomogeneous atmospheres: RRTM, a validated correlated-k model for the longwave. *J. Geophys. Res.*, **102**(D14), 16663-16682.

Morrison, J., W. Callendar, M. G. G. Foreman, D. Masson, and I. Fine, 2014: A Model simulation of future oceanic conditions along the British Columbia continental shelf. Part I: Forcing fields and initial conditions. *Atmos.-Ocean*, doi: 10.1080/07055900.2013.868340.

NIMR, 2012: Global climate change report corresponding to the IPCC fifth assessment report. National Institute of Meteorological Research 11-1360395-000341-10, Seoul, South Korea. 100 pp. (in Korean) [Availble online at http://www.climate.go.kr/home/cc_data/2013/climate-change_report_2012.pdf]

Oh, S. K., M. S. Suh, and D. H. Cha, 2013: Impact of lateral boundary conditions on precipitation and temperature extremes over South Korea in the CORDEX regional climate simulation using RegCM4. *Asia-Pac. J. Atmos. Sci*., **49**, 497-509.

_____, J. H. Park, S. H. Lee, and M. S. Suh, 2014: Assessment of the RegCM4 over East Asia and future precipitation change adapted to the RCP scenarios. *J. Geophys. Res. -Atmos*., **19**, 2913-2927.

Park, T., C. J. Jang, M. Kwon, H. Na, and K. Y. Kim, 2014: An effect of ENSO on summer surface salinity in the Yellow and East China Seas. *J. Marine Syst.*, doi: 10.1016/j.jmarsys.2014.03.017

_____, _____, J. H. Jungclaus, H. Haak, W. Park, and S. O. Im, 2011: Effects of the Changjiang river discharge on sea surface warming in the Yellow and East China Seas in summer. *Cont. Shelf Res.*, **31**, 15-22.

Sales, F. D., and Y. Xue, 2012: Dynamic downscaling of 22-year CFS winter seasonal hindcasts with the UCLA-ETA regional climate model over the United States. *Clim. Dynam.*, doi:10,1007/s00382-012-1567-x.

Sato, T., F. Kimura, and A. Kitoh, 2007: Projection of global warming onto regional precipitation over Mongolia using a regional climate model. *J. Hydrol*., **333**, 144-154.

Seo, K.-H., and J. Ok, 2013: Assessing future changes in the East Asian summer monsoon using CMIP3 models: Results from the best model ensemble. *J. Climate*, **26**, 1807-1817.

_____, _____, J.-H. Son, and D.-H. Cha, 2013: Assessing future changes in the East Asian summer monsoon using CMIP5 coupled models. *J. Climate*, **26**, 7662-7675.

Skamarock, W. C., J. B. Klemp, J. Dudhia, D. O. Gill, D. M. Barker, M. G. Duda, X-Y. Huang, W. Wang, and J. G. Powers, 2008: A description of the advanced research WRF version 3. *NCAR Technical Note NCAR/TN-475+STR*, National Center for Atmospheric Research, Boulder, Colorado, U.S.A., 123 pp. [Available online at http://www.mmm.ucar.edu/wrf/users/docs/arw_v3.pdf]

Sun, W-Y, K.-H. Kim, and J.-D. Chern, 2011: Numerical study of 1998 late summer flood in East Asia. *Asia-Pac. J. Atmos. Sci*., **47**, 123-135.

Trenberth, K. E., and C. J. Guillemot, 1995: Evaluation of the global atmospheric moisture budget as seen from analyses. *J. Climate*, **8**, 2255-2272.

Ueda, H., A. Iwai, K. Kuwako, and M. E. Hori, 2006: Impact of anthropogenic forcing on the Asian summer monsoon as simulated by eight GCMs. *Geophys. Res. Lett*., **33**, L06703, doi:10.1029/2005GL-025336.

Wang, B., J. Liu, H. J. Kim, P. J. Webster, and S. Y. Yim, 2012: Recent change of the global monsoon precipitation (1979-2008). *Clim. Dynam.*, **39**, 1123-1135.

_____, _____, _____, _____, _____, and B. Xiang, 2013: Northern Hemisphere summer monsoon intensified by mega-El Niño/southern oscillation and Atlantic multidecadal oscillation. *Proc. Natl Acad. Sci.*, **110**, 5347-5352.

_____, Z. Wu, J. Liu, J. Liu, C.-P. Chang, Y. Ding, and G. Wu, 2008: How to measure the strength of the East Asian summer monsoon. *J. Climate*, **21**, 4449-4463.

Watterson, I. G., 1998: An analysis of the global water cycle of present and doubled CO2 climates simulated by the CSIRO general circulation model. *J. Geophys. Res*., **103**, 23113-23129.

Yoshikane, T., F. Kimura, H. Kawase, and T. Nozawa, 2012: Verification of the performance of the pseudo-global-warming method for future climate changes during June in East Asia. *Sci. Online Lett. Atmos.*, **8**, 133-136.